ISSN 1063-7745, Crystallography Reports, 2013, Vol. 58, No. 5, pp. 743–748. © Pleiades Publishing, Inc., 2013.
Published in Russian in Kristallografiya, 2013, Vol. 58, No. 5, pp. 730–736.

SURFACE AND THIN FILMS

# Quantum Levitation of Nanoparticles Seen with Ultracold Neutrons*

**V. V. Nesvizhevsky[a], A. Yu. Voronin[b], A. Lambrecht[c], S. Reynaud[c], E. V. Lychagin[d], A. Yu. Muzychka[d], and A. V. Strelkov[d]**

[a] *Institut Laue-Langevin, 6 rue Jules Horowitz, F-38042 Grenoble, France*
*e-mail: nesvizhevsky@ill.eu*
[b] *Lebedev Institute, 53 Leninsky pr., RU-119991 Moscow, Russia*
[c] *Laboratoire Kastler-Brossel, CNRS, ENS, UPMC, Case 74, F-75252 Paris, France*
[d] *Joint Institute for Nuclear Research, 6 Joliot-Curie str, RU-141980 Dubna, Russia*

Received February 12, 2013

**Abstract**—Analyzing new experiments with ultracold neutrons (**UCNs**) we show that physical adsorption of nanoparticles/nanodroplets, levitating in high-excited states in a deep and broad potential well formed by van der Waals/Casimir-Polder (**vdW/CP**) forces results in new effects on a cross-road of the fields of fundamental interactions, neutron, surface and nanoparticle physics. Accounting for the interaction of UCNs with nanoparticles explains a recently discovered intriguing so-called "small heating" of UCNs in traps. It might be relevant to the striking conflict of the neutron lifetime experiments with smallest reported uncertainties by adding false effects there.

**DOI:** 10.1134/S1063774513050088

## INTRODUCTION

Surface diffusion of atoms, molecules and clusters, physically adsorbed in the potential well associated with van der Waals and Casimir-Polder interactions (**vdW/CP**) plays a key role in various phenomena in physics, chemistry, biology, and in applications [1–4]. The interaction is affected at small distance by "close-to-contact" effects depending on roughness and surface state [5, 6]. Because of experimental limitations, the precision studies are usually restricted to probes having either molecular or macroscopic sizes. Here we address the less extensively explored field of physical adsorption of nanoparticles and discover qualitatively new universal phenomena related to their sizes and masses. Rigorous theoretical formalism describing states of physically adsorbed nanoparticles and their interaction with ultra-cold neutrons (**UCNs**) [7–9] is given in a longer article [10]; however general features can be understood from arguments stated below. The depth of the potential well affecting the motion of a sufficiently small physisorbed particle near a surface is proportional to the number of atoms in it, while the thermal energy attributed to the particle does not depend on the number of atoms and equals $3k\_BT/2$, where $k_B$ is the Boltzmann constant and $T$ the temperature. Thus a nanoparticle is found near the surface in a deep and broad potential well in the normal direction. Nanoparticles in states with low quantum number n are strongly bound to the surface, therefore their motion along the surface is difficult because of roughness, surface defects, constrains, crystal steps, admixtures etc, which play a role of traps. Nanoparticles in high– $n$ states move easier along it, with the effects of roughness and inhomogeneities mixing the two velocity components. Nanoparticles in high-n states might form a two-dimensional "cloud". The number of states is so large that a nanoparticle exhibits typically a quasi-classical motion fitting the conditions searched for in [11, 33] for solving puzzles in UCN physics.

Here, we report on the theoretical justification for the existence of levitating nanoparticles, new treatment of the relevant existing UCN experimental data, and the results of new dedicated experiments, which provide evidence for levitating nanoparticles over solid and liquid surfaces. We show that our theoretical model describes all relevant existing and new UCN data. To our knowledge there is no alternative model, which could describe them. After a few reminders on the vdW/CP potential, we describe scattering of UCN on nanoparticles, discuss experimental results and consider consequences of our findings.

## THEORETICAL DESCRIPTION OF PHYSICALLY ADSORBED NANOPARTICLES

The shape of the potential is calculated using a general expression involving only the scattering properties of the two objects [12]. For example, the case of diamond nanospheres above a copper plane has been studied in great details in [13]. Electromagnetic waves scattering on a plate is characterized by Fresnel reflection amplitudes, the form of which is fixed by the dielectric response function ε of copper. For frequen-

* The article was translated by the authors.

cies ω lower than the plasma frequency $\omega_p$, copper behaves as a good reflector. For larger frequencies the reflection properties are poorer. When considering a nanoparticle of vanishing radius, the electric dipole approximation is sufficient. Calculations based on a simple model for the dielectric function of diamond containing only one resonance frequency $\omega_1$ reproduce the well-known vdW/CP energy. For distances small compared to the plasma wavelength (136 nm for copper), or the resonance wavelength (106 nm for diamond), the interaction reduces to the commonly used vdW formula with a power law $R^3/L^3$ in the vicinity of the surface, where $R$ is the nanoparticle radius, and $L$ the distance of closest approach to the plane.

For nanoparticles of arbitrary size the quantum dispersion energy must be calculated by integrating the phase-shifts corresponding to all modes of the electromagnetic vacuum. In particular, many Mie scattering amplitudes (corresponding to many multipole components beyond the electric dipole), contribute significantly to the effect when the particle is close to the surface [12]. The exact solution for the interaction energy predicts a smoother power law $R/L$ close to contact with the surface, thus leading to a regular solution for the Schrödinger equation, in contrast to the commonly used vdW formula.

We have analyzed the Schrödinger equation for the quantum dispersion potential and will sketch our findings here; details of the calculations are given in [10]. We found a large number of bound states with the eigenenergies $E_n$ deeper than the characteristic thermal motion energy $3k\_BT/2$. If nanoparticles are large enough, $R \sim 1$ nm, such states could be localized at distances of up to a few nanometers to the surface. The nanoparticle thus might fly over the surface while levitating in high–$n$ quantum states. More precise statements depend on the population and thermalization dynamics and are sensitive to the low–$n$ quantum states spectrum. In contrast to high– $n$ states, where the nanoparticles stay essentially far from the surface, the precise properties of low– $n$ states depend on close-to-contact details and in particular on the effect of roughness. Consequences of this effect can be characterized by using the methods developed for studying the Casimir force between two metallic plates. The probability of approach to close distances is reduced by contact repulsion from the highest peaks of the roughness profile [5], while the dispersion force is affected by the distribution of approach distances due to roughness [6]. Here we chose a simple parametric approach: on top of the attraction calculated in [6], we introduce contact repulsion so that the effective potential has a minimum at a distance equal to 1–3 nm for the solid samples used. Because of the large number of high–$n$ quantum states for the bound nanoparticles, a quasi-classical description of their motion in the vdW/CP potential is sufficient. Thus, when UCN bounce on the surface covered with levitating nanoparticles, we essentially deal with events of Doppler shift in UCN energy in the laboratory frame due to their elastic (in the centre-of-mass reference system) collisions with nanoparticles in high–$n$ quantum states.

## INTERACTION OF UCNS WITH PHYSICALLY ADSORBED NANOPARTICLES

Due to extremely low temperature of UCN (< 1 mK), small energy (<$10^{-7}$ eV), and low velocity (a few m/s) UCNs possess the unique property of total elastic reflection from motionless surfaces at any incidence angle. The probability of UCN loss per one bounce might be quite low: theoretically predicted probabilities of losses can as low as ~$10^{-9}$ (oxygen); the best experimentally achieved values are approaching ~$10^{-6}$ (oxygen, Fomblin). The dominant loss mechanisms are nuclear absorption of UCNs and up-scattering of UCNs on phonons in the surface material. Even at the ambient temperature the probability of up-scattering is much smaller than the probability of coherent elastic reflection. That is why UCNs can be stored in closed traps for extended periods thus providing an extremely sensitive probe for rare processes or weak interactions. When studying UCNs storage in traps, unusual inelastic scattering of UCNs on trap surfaces was discovered [14–18]. One calls this phenomenon "small heating of UCNs" and such up-scattered neutrons Vaporizing UCNs (**VUCN**) in analogy to vaporization of molecules. First measurements were followed by studies of several research groups, which essentially confirmed the initial observation, but suggested controversial estimations of the VUCNs production rates.

Let us first give strong experimental motivation for the existence of levitating nanoparticles above surfaces. In the following we will show VUCN spectra that we calculated with a method sketched below using the initial UCN spectrum and the spectrometer spectral efficiency that we had measured experimentally. It has been found in [18] that the count rate of VUCN produced on stainless steel surfaces shows a sharp increase as a function of the sample pre-heating temperature, the so-called "temperature resonance" shown in the left part of Fig. 1. On the right part of Fig. 1 we show the surface density of nanostructures measured with an Atomic Force Microscope (**AFM**) as a function of temperature. These measurements indicate an intense formation of nanostructures on the surface which takes place precisely at the temperature of sharp increase in the VUCN count rate. Nanostructures' size increases monotonously as a function of the heating temperature: a few particles at the ambient temperature, intense growth of the number and size of nanostructures below 350°C; further increase in size but decrease in number of nanoparticles above 350°C (some nanoparticles coagulate). While no alternative

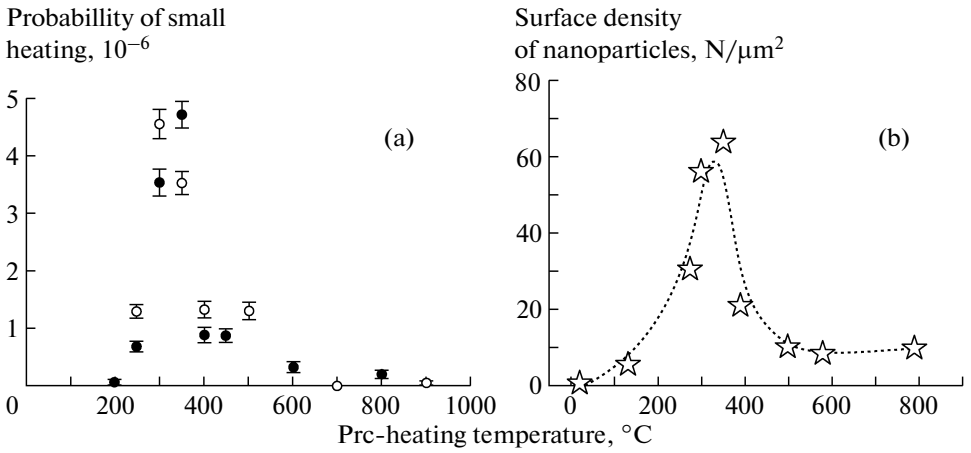


**Fig. 1.** (a) The probability of small heating of UCNs on surface of stainless steel samples is shown as a function of the temperature of sample outgasing (pre-heating); the measurement is performed at 300 K. Black and white points show results of two independent experiments using analogous samples. (b) The surface density of nanostructures with a radius of 6–7 nm (stars) corresponding to the resonance enhancement in the efficiency of VUCN detection, observed in AFM. More details in the body text.

explanation has yet been proposed, we regard this as an indication that it is due to levitating nanoparticles.

Let us now briefly describe the basic equations of our model. The average differential cross-section of the interaction of an UCN with a nanoparticle is [10]:

$$\frac{d\bar{\sigma}}{dE} = \frac{1}{2mk_n}\left(\frac{M}{2\pi k_B T}\right)^{3/2} \times \int_0^\infty dV \exp\left(-\frac{MV^2}{2\pi k_B T}\right) \int_{k_{\min}}^{k_{\max}} dk_0 \int_0^{2\pi} d\varphi \left|f_B(k_0, V, E, \varphi)\right|^2, \quad (1)$$

with $m$, $v_n$, $k = mv_n$ the neutron mass, initial velocity and momentum and $M$ and $V$ the nanoparticle mass and velocity. The kinematically allowed area of integration $[[k_{\min}, k_{\max}]]$ is determined by the conditions

$$\begin{cases} |mV - k_n| \le k_0 \le mV + k_n \\ \left|\sqrt{k_n^2 + 2mE} - mV\right| \le k_0 \le \left|\sqrt{k_n^2 + 2mE} + mV\right|, \end{cases} \quad (2)$$

$E$ is the energy transfer and $k_0 = m\left|\bar{v}_n - \bar{V}\right|$ the incident momentum modulus in the center-of-mass reference system. The Born amplitude $f_B$ of the neutron nanoparticle scattering is $f_B(q) = -2mRU_0/q^2\left[\hbar\sin(qR/\hbar)/(qR) - \cos(qR/\hbar)\right]$ where $q$ is the transferred momentum, and $U_o$ is the nanoparticle-neutron optical potential. To estimate relevant nanoparticle radii, we use the above formalism and follow the general approach from [11]: 1— $R$ should not be too small, otherwise the coherent interaction cross-section is too low (as $d\bar{\sigma}/dE \sim R^6$), and 2— $R$ should not be too large, otherwise nanoparticles are too heavy; thus their thermal velocity is too small, $q$ is too small, and VUCNs could not be found in the window of efficient VUCN detection.

We first apply our method to the small heating of UCNs on solid surfaces, where we have estimated in several manners the effective radius $\bar{R}$ of nanoparticles contributing to the observed inelastic process. The first sample [16, 17] we consider is powder of diamond nanoparticles with radii of 1–10 nm, on a copper surface, or above "sand" of diamond nanoparticles. We estimate the effective radius by the following three methods. 1—Using measured shapes of the differential VUCN spectra leading to $\bar{R}^{spectrum}_{diamond} = 9.4 \pm 0.4$ nm. 2—Using measured temperature dependencies of the count rates of detected VUCNs which gives $\bar{R}^{temp}_{diamond} = 9.5 \pm 0.6$ nm; 3—Using the measured size distribution of nanoparticles: $\bar{R}^{aver.\ size}_{diamond} = 8.5 \pm 0.5$ nm. Agreement between these independent estimations is convincing keeping in mind that they are not very sensitive to such parameters as the nanoparticle size and shape distribution, clustering, surface roughness, impurities etc. In contrast, if one abandons the "free levitation" model and "tunes" one critical parameter alone in the formulas given above, say $R$, by 10–20%, theoretical predictions largely contradict the data. Strictly speaking, there is no reason then, why all these estimations of $R$ are equal, or even comparable. Another measured sample is nanoparticles appearing on stainless steel surface due its thermal treatment [17, 18]. Again, the two independent estimations of the effective radii $\bar{R}^{spectrum}_{stainless\ steel} = 6.3 \pm 0.3$ and $\bar{R}^{aver.\ size}_{stainless\ steel} = 6.6 \pm 0.3$ agree. The effective masses of diamond and stainless steel nanoparticles estimated above are equal, thus providing an additional test of validity of our model.

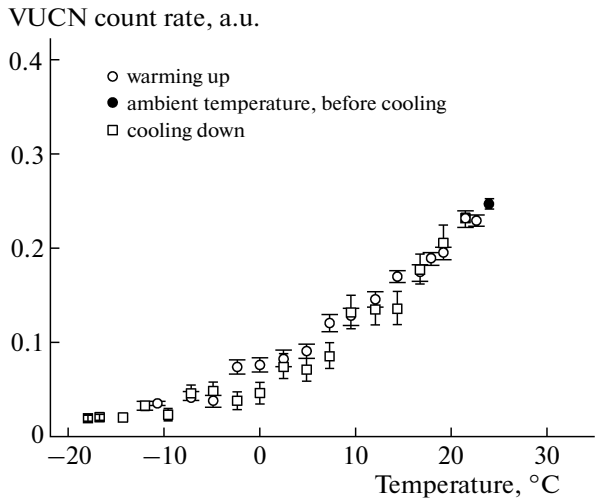


**Fig. 2.** VUCN count rate in a.u. on a Fomblin HVAC 18/8 surface as a function of temperature. The circle indicates the data at ambient temperature (the total probability of small heating is $10^{-5}$ per wall collision); open squares show data measured when cooling the sample down, and open circles correspond to data measured when warming the sample up.

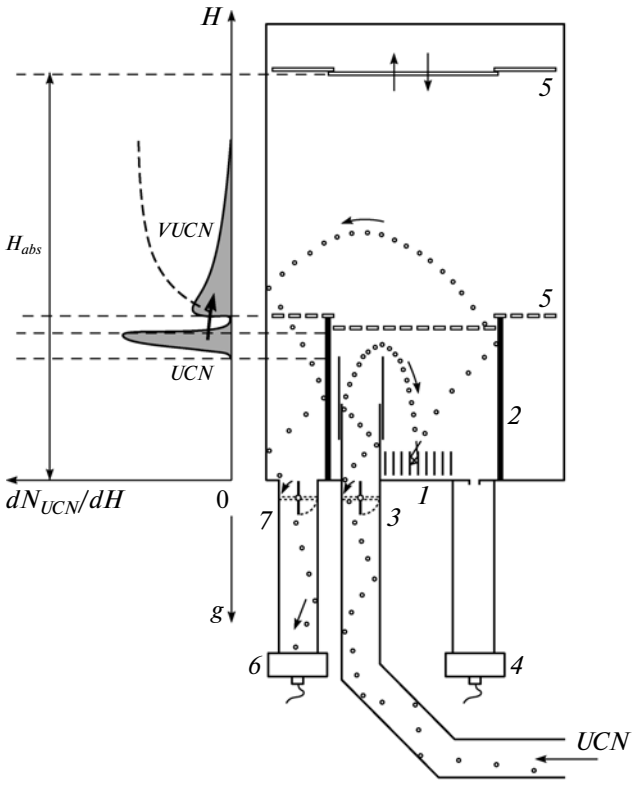


**Fig. 3.** Layout of the Big Gravitational Spectrometer (**BGS**): (*1*) sample, (*2*) gravitational barrier, (*3*) entrance valve, (*4*) UCN monitor detector, (*5*) UCN absorber, (*6*) VUCN detector, and (*7*) exit valve. The principle of the procedure to measure small energy transfers is sketched in the insert on the left side. From bottom to top (in scale): initial differential UCN spectrum (the mean energy is 31 neV, the half-width of the spectral mono-line is 3 neV), a dead-zone of 3neV insensitive to VUCNs, the differential and integral (dashed line) spectra of VUCN. The differential efficiency of VUCN detection is calculated using precisely measured values of UCN and VUCN storage times as a function of their energy; decrease in the detection efficiency, caused by partial losses of neutrons in samples, is taken into account.

Small heating of UCN on liquid Fomblin oils has been observed as well [14–16] but no detailed spectral measurements have been performed. In view of the above evidence we assume that this phenomenon might be due to collisions of UCNs with levitating Fomblin oil nanodroplets. This mechanism would complement the known effects due to surface capillary waves [19] and surface thermal fluctuations [20]. We mention but not analyze here other hypotheses on origin of VUCN [21–23]; as they do not provide quantitative predictions and/or do conflict with experiments. While solid nanoparticles are characterized by long formation and evolution times, the number and size of levitating liquid nanodroplets [31, 32] could rapidly change with temperature, or other conditions like pressure, as they are governed by equilibrium of permanent formation of nanodroplets from vapors, and of their evaporation and coagulation.

To compare these models, we measured VUCN count rates as a function of temperature, shown in Fig. 2. Although our model does not describe explicitly the number of nanodroplets as a function of temperature, it is natural to assume that this number decreases with falling temperature as the Fomblin oil vapor pressure above surface, in analogy to the present data. Alternative interpretations of neutron small-heating, such as the hypothesis of thermal fluctuations of the surface [20], and the hypothesis of capillary surface waves [10], seem to contradict these experimental results, as they propose either too low absolute probabilities [20], or/and inverse temperature dependence of the probability [19]. In contrast, our model gives the correct qualitative behavior and reasonable values.

In order to assess this question more precisely we have calculated the VUCN spectrum within our model and compared it to results of a new dedicated precision study of small heating of UCNs on solid and liquid surfaces in our precisely calibrated spectrometer BGS shown in Fig. 3. Measurements of small changes in energy of UCN in this spectrometer are based on the following principle. The energy of UCN is defined by the height of its maximum raise in the Earth's gravitational field; thus it can be expressed in energy or height units. Using an absorber placed above the storage vessel, and a neutron guide entering the vessel at some height above its bottom, one can form a narrow UCN energy line with the mean energy 31 neV and the half-width 3 neV. The maximum energy in this mono-line is below the height of the gravitational barrier by 3 neV. If the energy of UCN increases during their storage

(they are "converted" into VUCN), such neutrons can overcome the gravitational barrier and reach the detector. The differential efficiency of VUCN detection is calculated using precisely measured values of storage times of UCN and VUCN, as a function of their energy.

The comparison is shown in Fig. 4 for several different physical systems, i.e. ultra-diamond ($\overline{R} \sim 2.5$ nm) and sapphire ($\overline{R} \sim 10$ nm) nanoparticles with broad size distribution, thin (1 μm) and thick (a few mm) layers of Fomblin oil HVAC 18/8, and naturally growing nanoparticles on a copper surface. We calculated integral VUCN spectra and corresponding VUCN count rates as a function of the absorber height taking into account the measured differential spectrometer efficiency. Clearly all integral spectra are equivalent within statistical accuracy showing that there is a universal behavior for these very different physical systems. This is a natural consequence of our model. In fact, the sensitivity of the spectrometer is sharply shaped to some nanoparticle mass, which, in turn, depends on the initial UCN energy range and the window of the spectrometer sensitivity. However, within the peak resonance sensitivity, there is a slight dependence on the mass distribution, which we show in Fig. 4. If the size distribution is known, the corresponding uncertainties are small. Note that our simplified model assumes at this stage that UCN scatter on spherical uniform and distant nanoparticles; rotations, precise shape and non-uniformity of nanoparticles, as well as effects of interference with surface are disregarded here. Concerning the results for Fomblin oil, they give evidence that the dominant mechanism of small heating of UCN on Fomblin oil surface in our experiment is UCN scattering on levitating nanodroplets.

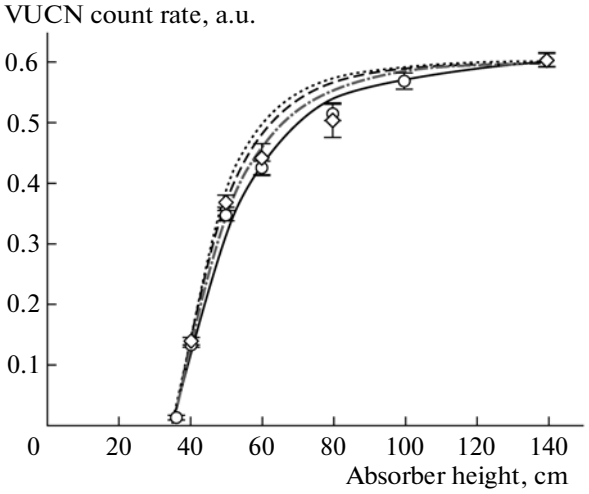


**Fig. 4.** VUCN count rate as a function of neutron energy, expressed in UCN raising height in the Earth's gravitational field, in cm. Circles show results measured with various solid nanoparticles: diamond, sapphire, copper; all these results agree within statistical accuracy. Rhombi indicate data measured with a Fomblin oil sample; they agree with the data on solid nanoparticles. Four lines correspond to our model calculations of VUCN spectra on the Fomblin surface, for four hypotheses on the size distribution of nanodroplets: $((R/R_0)^{-l}$ where $l = 1, 2, 3, 4$ from top to bottom. The lines and the data are normalized to equal count rate at infinite height.

## CONCLUSION

The present study was motivated in part by the unsatisfactory status of the neutron lifetime $n$ experiments which show large and so far unexplained discrepancy between results with smallest reported uncertainties [24–26]. This contradiction has been discussed with far-reaching consequences of an eventual shift of the mean world value for fundamental particle physics and cosmology [27–29], but only a single study has tried to verify independently the validity of the measured results [30]. All these experiments use UCN traps with Fomblin-oil walls, and assume conservation of UCN energy. However using our data and model, it is easy to show that a major fraction of UCNs do change their energy, so that their loss rate is different from the assumed values and major false effects might arise. In particular, as the rate of forming Fomblin-oil nanodroplets depends on experimental conditions, the basic idea of these experiments is compromised: the geometrical and energy methods of UCN loss extrapolation cannot be applied without reservations. Nanodroplets production rates depend on parameters not properly controlled like pre-history of the Fomblin oil treatment or vacuum. In particular, the UCN loss probability would be different in large and small traps; it would also evolve in time. The task of estimating reliable corrections to $n$ values goes beyond the scope of this article.

An attractive application might consist in studying vdW/CP interaction between levitating nanoparticles and surfaces. Corresponding corrections to the integral VUCN spectra account for ~10% even in the present study, and could be increased due to optimization of experimental parameters. Surface potentials define distances of levitating nanoparticles to surfaces. As UCN can scatter inelastically twice on the same nanoparticle, before reflection from the surface and after reflection, VUCN spectra are affected by distances of nanoparticles to the surface.

Adsorption of atomic clusters is used for decorating surface defects, boundaries, step edges, grain boundaries, and elastic strain fields. In contrast, UCNs are sensitive to nanoparticles in motion above defect-free zones, thus giving us access to nanoparticle mobility. In levitation, nanoparticle mobility is very high; on the other hand chemical interactions largely reduce it thus giving us access to chemical properties of nanoparticles and surfaces. In an analogous way, one could also measure electrostatic effects.

## ACKNOWLEDGMENTS

We thank our colleagues for useful discussions and help, in particular A.L. Barabanov, S.T. Belyaev, H.G. Boerner, L.N. Bondarenko, T. Brenner, D. Delande, D. Dubbers, P. Geltenbort, R. Golub, V.K. Ignatovich, A. Leadbetter, S.K. Lamoreaux, V.I. Morozov, G.V. Nekhaev, S. Paul, J.M. Pendlebury, G. Pignol, and K.V. Protasov, also RFFI for partial financial support of this work in framework of grant 13–02–00657 A. The authors benefited from exchange of ideas within the ESF Research Network CASIMIR, and the GRANIT collaboration.

## REFERENCES

1. K. Oura, V. G. Lifshits, and A. A. Saranin, *Surface Science: An Introduction* (Bergin-Verlag, Berlin, 2003).
2. K. W. Kolasinski, *Surface Science: Foundations of Catalysis and Nanoscience* (Wiley, Chichester, West Sussex, 2008).
3. G. Antczak and G. Ehrlich, Surf. Sci. Rep. **62**, 39 (2003).
4. E. Shustorovich, *Metal-Surface Reaction Energetics: Theory and Applications to Heterogeneous Analysis, Chemisorption, and Surface Diffusion* (VCN, 1991).
5. P. G. van Zwol et al., Phys. Rev. B **80**, 235401 (2009).
6. W. Broer et al., Eur. Phys. Lett. **95**, 30001 (2011).
7. V. I. Luschikov, Yu. N. Pokotilovsky, A. V. Strelkov, and F. L. Shapiro, JETP Lett. **9**, 23 (1969).
8. V. K. Ignatovich, *The Physics of Ultracold Neutrons* (Clarendon, Oxford, 1990).
9. R. Golub, D. J. Richardson, and S. K. Lamoreux, *Ultra-Cold Neutrons* (Higler, Bristol, 1991).
10. V. V. Nesvizhevsky, A. Yu. Voronin, A. Lambrecht, and S. Reynaud, New J. Phys. **14**, 093053 (2012).
11. V. V. Nesvizhevsky, Phys. At. Nucl. **65**, 400 (2002).
12. A. Canaguier-Durand et al., Phys. Rev. Lett. **102**, 230404 (2009).
13. A. Canaguier-Durand et al., Phys. Rev. A **83**, 032508 (2011).
14. V. V. Nesvizhevsky et al., Eur. J. Appl. Phys. **6**, 151 (1999).
15. A. V. Strelkov et al., Nucl. Instrum. Methods Phys. Res., Sect. A **440**, 695 (2000).
16. L. Bondarenko et al., JETP Lett. **68**, 691 (1998).
17. E. V. Lychagin et al., Phys. At. Nucl. **65**, 1995 (2002).
18. D. G. Kartashov et al., Int. J. Nanoscience. **6**, 501 (2007).
19. S. K. Lamoreaux and R. Golub, Phys. Rev. C **66**, 044309 (2002).
20. A. L. Barabanov and S. T. Belyaev, Eur. Phys. J. B **15**, 59 (2000).
21. A. Stepaniants et al., J. Low Temp. Phys. **113**, 1159 (1999).
22. S. S. Malik et al., Phys. Lett. A **260**, 328 (1999).
23. Y. N. Pokotilovki, Eur. Phys. J. B **8**, (1999) 1; Phys. Lett. A **255**, 173 (1999); JETP Lett. **69**, 91 (1999).
24. S. Arzumanov et al., Phys. Lett. B **483**, 15 (2000).
25. A. P. Serebrov et al., Phys. Lett. B **605**, 72 (2005).
26. A. Pichlmaier et al., Phys. Lett. B **693**, 221 (2010).
27. H. Abele et al., Phys. Rev. Lett. **88**, 211801 (2002).
28. D. Dubbers and M. G. Schmidt, Rev. Mod. Phys. **83**, 1111 (2011).
29. G. J. Mathews et al., Phys. Rev. D **71**, 021302 (2005).
30. S. Paul, Nucl. Instrum. Methods Phys. Res. **611**, 157 (2009).
31. K. Koga et al., J. Chem. Phys. **109**, 4063 (1998).
32. T. Tadros et al., Adv. Col. Interface Sci. **108**, 108 (2004).
33. V. K. Ignatovich, Nucl. Instrum. Methods Phys. Res., Sect. A **440**, 709 (2000).